Asian Journal of Water, Environment and Pollution, Vol. 20, No. 6 (2023), pp. 67-75.
DOI 10.3233/AJW230081

Kinetic, Isotherm, and Thermodynamic Modeling of Pb(II) Heavy Metals Removal from Aqueous Solutions Using Hydrogel-MWCNTs Nanocomposites

Zainab R. Maktof and Nadher D. Radia[1]*

Thi-Qar General Directorate of Education, Ministry of Education, Thi-Qar, Iraq
[1]Department of Chemistry, College of Education, University of Al-Qadisiyah, Al-Qadisiyah, Iraq
✉ nadhir.dhaman@qu.edu.iq

Received July 11, 2023; revised and accepted October 18, 2023

Abstract: This study investigated the ability of nanocomposite hydrogels (NaCMC-g-AAc/COOH-MWCNTs) to adsorb Pb(II) ions, an environmental pollutant. The characterisation of the hydrogel and nanocomposite was achieved using FTIR, FESEM, XRD and TGA techniques, XRD techniques. Adsorption studies showed that equilibrium was reached after 120 minutes with a removal efficiency of 82%. Many factors were also studied, as the results indicated that the adsorption equality was of the (S4) type according to Giles' classification, and the adsorption parallels for Pb (II) ions matched the Freundlich adsorption model. The absorption process was found to be endothermic, with absorption increasing with increasing temperature. Positive content and entropy are noted, as well as negative free energy, indicating the physical and spontaneous nature of the process.

Key words: Adsorption, lead (II), oxidised multi-wall carbon nanotubes, sodium carboxymethyl cellulose.

Introduction

The adverse effects of water pollution on human health and the environment are well-established, with a particular focus on the role of heavy metal ions such as Pb (II). These significant environmental pollutants pose potential health risks, particularly within water resources, due to their high toxicity and non-biodegradability (Al-Mashhadani et al., 2021; Thibaut, et al., 2016). Recognised particularly in industries such as metal plating, tanneries, oil refining, and mining, Pb (II) often permeates into soil and water systems, contributing to bioaccumulation along food chains and significant health risks, including effects on red blood cells, the nervous system, and kidneys (Lin et al., 2000). Addressing Pb (II) pollution, given its resistance to biological degradation, is therefore of utmost importance, not only for the sustainability of aquatic life but also for those relying on water resources. Several methodologies for Pb (II) removal from aqueous solutions have been developed, encompassing techniques such as ion exchange, precipitation, reverse osmosis, and notably adsorption (Mohsen et al., 2015). Adsorption, a cost-effective technique recognised for its efficiency, simplicity, and potential for reusing adsorbents, has been gaining considerable attention (Aljeboree and Alkaim, 2019). Recent advances in this field have particularly explored the use of hydrogel surfaces decorated with multi-walled carbon nanotubes (MWCNTs), noted for their superior adsorption performance (Kumar et al., 2019; Sandeep and Suresha., 2013). Owing to their high surface area, chemical stability, and tunable surface functionality, MWCNTs have demonstrated their potential in enhancing the adsorption capacity of hydrogels (Radia et al., 2022). Hydrogels, with their high water content, biocompatibility, and ease

*Corresponding Author

of functionalisation, have been recognised as an ideal platform for MWCNT incorporation (Assadi et al., 2016). Despite the significant progress made, gaps in understanding remain. These encompass the preparation processes of these hybrid materials and the mechanisms underlying lead ion adsorption, which require further exploration to optimise performance and understand the associated physicochemical interactions (Aljeboree et al., 2019; Alvares Rodrigues and Pinto da Silva, 2010). The current study addresses these gaps, providing an in-depth review of the use of hydrogel surfaces embedded with MWCNTs for lead ion removal from aqueous solutions (Radia et al., 2022).

Materials and Methods

Materials

NaCMC (99.9%), AAc (99.9%), COOH-MWCNTs (multi-walled carbon nanotubes oxidised), KPS (98%), N,N-methylenebisacrylamide (MBA) 98%, lead(II) nitrate ($PbNO_3$), NaOH and HCl (98%) are all used in this work. Each one was an authentic Merck product. Reagents of analytical quality did not require further purification. Deionised water was used in the solution-making process to ensure analytical purity.

Synthesis of (NaCMC-g-pAAc) and (NaCMC-g-AAc)/COOH-MWCNTs Composite

Typically, 1g of CMC is weighed and dissolved in 25 mL of deionised water. To this mixture, appropriate amounts of AAc 1.5 g added periodically, MBA (prepared by dissolving 0.075 g in 2 mL of distilled water), and KPS (prepared by dissolving 0.05 g in 2 mL of distilled water) are added under vigorous stirring, maintaining the total volume at 30 mL. An optimal amount of 0.004 g of o-MWCNTs is sonicated with 2 mL of deionised water for about 60 minutes. This solution is then added to the reaction mixture in a 100 mL beaker containing CMC, AAc, MBA, and KPS, with continuous stirring. The reaction mixture is then heated at 70°C for 3 hours in a water bath. The resulting product is cut into small pieces and washed with deionised water to remove any unreacted materials. The (CMC-g-AAc)/COOH-MWCNTs nanocomposite hydrogel is then dried in an oven at 70°C for approximately 24 hours. Hydrogels were prepared by the same steps as above without the addition of COOH-MWCNTs. Finally, it is ground to a fine powder, as shown in Figure 1.

Characterisation of Adsorbents

FTIR spectroscopy was used to identify the active functional groups in the hydrogels and NaCMC-g-p(AAc)/COOH-MWCNTs nanocomposite hydrogels, as well as to identify any transitions or changes after lead ion adsorption, within the wavelength range 400–4000 cm^{-1}. The samples were mixed with potassium bromide (KBr) and then pressed. XRD technique was used to identify the crystalline properties such as crystalline nature, crystalline size, and distances between the hydrogels and surfaces of the prepared NaCMC-g-p(AAc)/COOH-MWCNTs nanocomposite hydrogels. FESEM was used to determine the external structure of the crosslinked hydrogel prepared before and after Pb(II) adsorption, in terms of size, shape and pores. It was used with different amplification powers under a voltage of 8000 kV. A thermogravimetric analysis (TGA) technique was used to determine the stability of the NaCMC-g-p(AAc)/COOH-MWCNTs hydrogel and nanocomposite hydrogel. It was used by tracking the change in mass of a sample resulting from slow and continuous heating within a temperature range of 30-800℃.

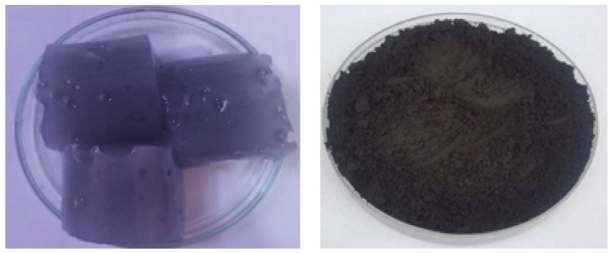

Figure 1: (NaCMC-g-pAAc)/COOH-MWCNTs nanocomposite hydrogel.

Adsorption Isotherm

In order to investigate the equilibrium isotherms for the Pb(II) ion, solutions with varying concentrations of the Pb(II) ions (100-1000 ppm) were prepared. Subsequently, 0.05 g of the adsorbent was added to 10mL of each solution and placed in a controlled shaking device at 25°C and at a speed of 120 rpm for 120 minutes, in order to reach equilibrium. The absorbance of each solution was then measured at the maximum wavelength, λ_{max} = 283nm, after being separated using a centrifuge at 6000 rpm for 15 min. This was accomplished using an atomic absorption photometer. The quantity of lead (II) ions adsorbed onto the prepared surface was calculated using the following equation (Zheng et al., 2019):

$$Q_e = \frac{m(C_o - C_e)}{V_{sol}} \quad (1)$$

$$Re\% = \left(\frac{C_o \times C_e}{C_o} \right) \times 100 \quad (2)$$

In this equation, Q_e represents the quantity of adsorbed substance, C_o is the initial concentration, C_e is the concentration at equilibrium, V_{sol} is the solution volume, and m represents the weight of the adsorbent.

Influence of Temperature

The adsorption experiment was repeated under variable temperature conditions (20, 25, 30 and 35°C) to calculate the essential thermodynamic functions associated with the process. The temperature variation provided a nuanced understanding of how changes in thermal conditions affect the adsorption mechanism and efficiency.

Effect of pH

The adsorption experiment was also conducted as a function of pH, utilising a stable concentration of metal ions. Adjustments to the pH, within a range of 3 to 10, were achieved using hydrochloric acid and sodium hydroxide. The pH of the suspensions was measured at the beginning and conclusion of the adsorption process using a pH meter. These measurements elucidated the role of pH in the adsorption process, confirming previous findings that pH can significantly influence adsorption effectiveness.

Results and Discussion

FTIR the application of infrared spectroscopy enabled the characterisation of functional group interactions and their spatial diagnosis in the beam. As shown in Figure 2 (i), the Fourier Transform Infrared Spectroscopy (FTIR) data for NaCMC, which reveals a broad absorption peak at 3319 cm^{-1}, signaling the presence of hydrogen-bonded O-groups. Absorption bands witnessed at 1718, 1460, and 1402 cm^{-1} are attributable to the stretching vibration of the C=O from the carboxylate group. Polysaccharide-associated absorption bands also emerge at 1410 cm^{-1} and 1023 cm^{-1}, linked to C–H bending and CO bond stretching, respectively. With respect to NaCMC-pAAc hydrogel and NaCMC-pAAc/COOH-MWCNTs, an amplification of the characteristic band's intensity at 1402 cm^{-1} is noticed, hinting at the symmetric stretching mode of the carboxylate group and corroborating the formation of the hydrogel. Additional peaks at 1537 cm^{-1} were related to the C=O asymmetric stretching of carboxylate anions in AA units. Additionally, a broad absorption peak at 3319 cm^{-1} for NaCMC evolved into a hump at 3142 cm^{-1} in the broad absorption peak after AA surface modification. These findings suggest successful AA copolymer grafting onto the CMC (Figure 2 ii-iii).

The nanocomposite hydrogel's FT-IR spectrum (CMC-g-AAc/COOH-MWCNTs) featured a broadband within the 3250-3427 cm^{-1} range, suggestive of H-N and H-O carboxylic band interference. CH_2 bonds in aliphatic compounds were identified at 2427 cm^{-1}. A 1743 cm^{-1} band, attributable to the carbonyl group of carboxylic acid, was also detected. Further, C-C and C-O groups were discerned at 1164 cm^{-1} and 1018 cm^{-1} respectively, and C–H group bending was noticed within the 500-813 cm^{-1} range. Post adsorption, a shift in the characteristic peaks' location was observed in the NaCMC-g-pAAc/COOH-MWCNTs nanocomposite hydrogel FTIR, along with the emergence and disappearance of some peaks (Plans et al., 2015; Ricci et al., 2015). The FT-IR spectrum after the adsorption process of Pb(II) ions on the surface of NaCMC-g-pAAc/COOH-MWCNTs indicates that Pb(II) ions are bonded to the amine groups, affecting their vibrations. The ionic bond results in a decrease in transmittance when adsorption occurs. Also, Pb(II) ions affect the stretching and bending of the OH and C-H groups, which indicates changes in the positions of hydroxyl, amino, and carbonyl groups

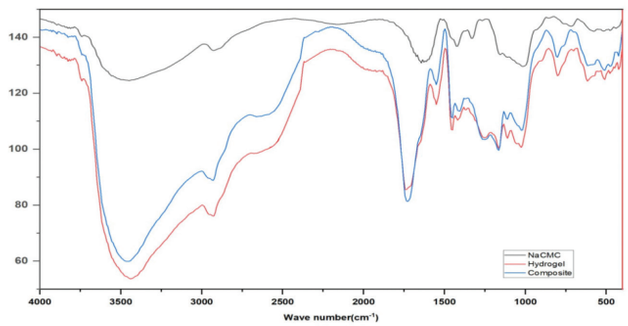

Figure 2: FT-IR of (i) NaCMC, (ii) hydrogel, and (iii) hydrogel nanocomposite.

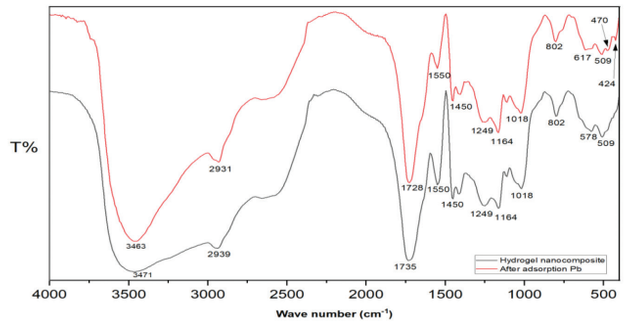

Figure 3: FT-IR of (NaCMC-g-AAc)/COOH-MWCNTs nanocomposite hydrogel and after adsorption Pb(II) ions.

during the absorption of these ions, as shown in Figure 3. This observation can support the proposed mechanism of Pb(II) ion adsorption on the surface of the NaCMC-g-pAAc/COOH-MWCNTs composite. The changes in the vibrational modes of these functional groups suggest their involvement in the adsorption process, indicating possible interactions between Pb(II) ions and these groups (Angevaare et al., 1990).

Analysis of FE-SEM

The Field Emission Scanning Electron Microscopy (FE-SEM) technique was employed to investigate the surface properties of (NaCMC-g-pAAc) hydrogel and (NaCMC-g-pAAc)/COOH-MWCNT, permitting evaluation of particle shape, size, aggregation, and surface nature (porous or smooth). Furthermore, surface distribution and interaction among polymer chains were assessed. High-resolution FESEM images revealed that the hydrogel (NaCMC-g-pAAc) displays a highly porous and interconnected network structure with a broad range of pore sizes. The pores appeared irregular in shape, reflecting the heterogeneous nature of the hydrogel as illustrated in Figure (4a). The prepared composite (NaCMC-g-pAAc)/COOH-MWCNT, as shown in the

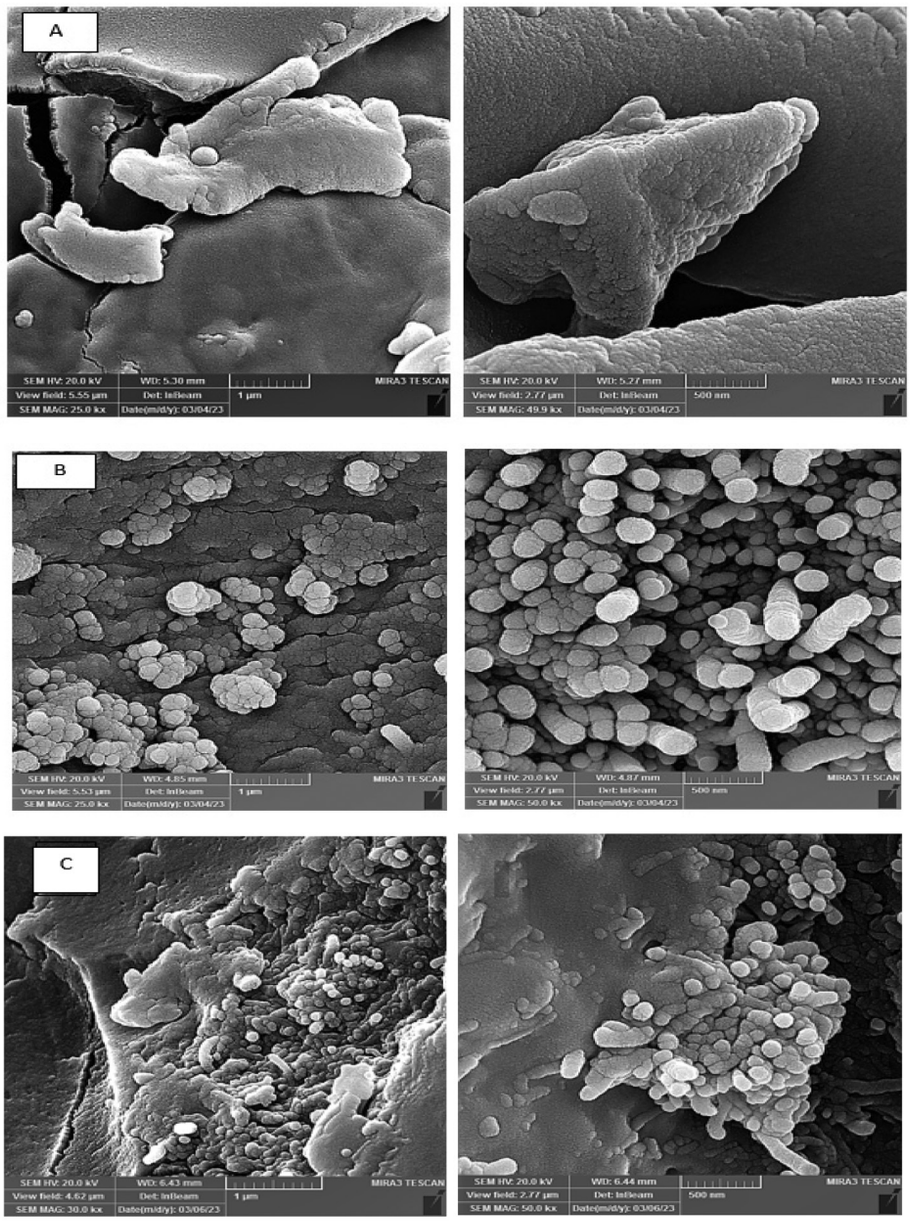

Figure 4: SEM images of (A) NaCMC/p(AAc) hydrogel. (B) NaCMC-g-AAc/COOH-MWCNTs nanocomposite hydrogel. (C) (NaCMC-g-AAc)/COOH-MWCNTs nanocomposite hydrogel after adsorption of Pb(II).

FE-SEM images depicted in Figure (4b), demonstrated a surface that is smooth, clear, porous, with a sponge-like structure, layered network, and increased surface roughness and porosity with an irregular structure. The surface morphology also indicated the dispersion of carbon nanotubes evenly throughout the hydrogel due to the presence of functional groups on the surfaces of the carbon nanotubes and the hydrogel, and the van der Waals forces bonding the polymer layers together. Upon the adsorption of Pb (II) ions onto the surfaces of the composite, FE-SEM images, as displayed in Figure (4c), revealed that the composite surfaces become less porous following the adsorption process. This observation can be attributed to the presence of elemental ions on the surfaces of the composite and their attachment to the active sites of the prepared compounds, indicating the occurrence of the adsorption process (Havrdová, et al., 2014; Okamoto and Meshitsuka, 2003).

Analysis of XRD

The XRD spectrum of the hydrogel and composite showed broad bands within 2θ (15-30) degrees for the hydrogel, and 2θ (14-43)° for the composite hydrogel, suggesting their amorphous chemical structures. Sharp, high beams at 2θ = 20.038 (hydrogel) and 2θ = 20.888 (compound) further confirmed this (Figure 5).

Analysis of TGA

Weight loss in three stages was revealed by the hydrogel's TGA curve, which is attributable to increasing temperature (Figure 6). The first stage, with a 19.47% weight loss between 50 and 250°C, was due to the loss of water molecules or moisture. The second and third stages, with a 53.95% weight loss between 250 and 550°C and a 9.987% loss between 550 and 800°C, respectively, were attributed to decarboxylation and CO_2 gas release, and hydrogel chain degradation. For the (NaCMC-g-pAAc)/COOH-MWCNTs nanocomposite hydrogel, the TGA curve showed four stages of gradual weight loss with increasing temperature. The stages involved 5.211% loss between 50 and 150°C (moisture loss), 24.62% loss between 150 and 250°C (decarboxylation and CO_2 release), 44.81% loss at 250-500°C (glycosidic bond split and saccharide ring desiccation), and 6.146% loss between 500 and 800°C (crosslink decomposition in the polymer) (Sabri, 2020).

Effect of Adsorbent Weight

Different amounts of the manufactured adsorbent surface were tested to see how they affected the

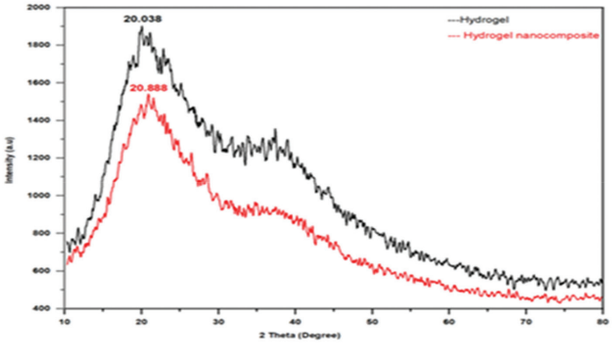

Figure 5: XRD spectra of NaCMC-g-p(AAc) hydrogel and (NaCMC-g-AAc)/COOH-MWCNTs nanocomposite.

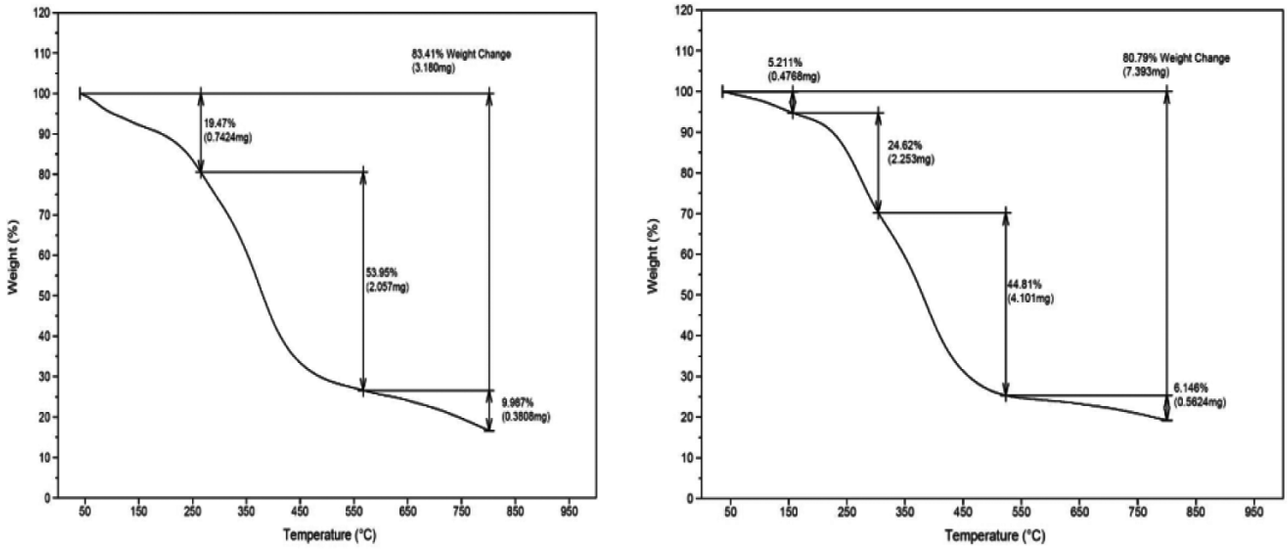

Figure 6: (A) TGA of NaCMC-g-p(AAc) hydrogel, (B) TGA of (NaCMC-g-pAAc)/COOH-MWCNTs nanocomposite hydrogel.

adsorption of the Pb (II) ions, which would indicate the ideal adsorbent weight. To do this, different amounts of the produced gel (from 0.01g to 0.11g) were dipped into 10 mL of a 1000 ppm lead (II) ions solution. The samples were shaken for 120 minutes at 25°C and 120 revolutions per minute in a controlled apparatus. The solutions were then centrifuged at 6000 rpm for 15 minutes to separate them. Therefore, the ideal weight affecting the adsorption of the Pb (II) ion may be determined by plotting the removal percentage of adsorbate versus the weight of the adsorbent surface and that a removal efficiency (Re%) of 82% of Pb(II) has been attained as shown in Figure 7.

Adsorption Isotherm

For adsorption isotherm experiments, lead Pb(II) concentrations ranged from 100 to 1000 mg/L. The effect of contact time and equilibrium concentration was evaluated at 25 °C. After the adsorption process, the aliquots were filtered and the concentration was measured using an Atomic Absorption Photometer. The adsorption ratio and adsorption capacity (q_e) were determined using Equations 1 and 2, respectively, and then the well-known isothermal equation models, Freundlich, Langmuir and Timken, were applied to the data obtained from the adsorption of lead Pb(II) onto the composite. Surface (NaCMC-g-pAc/COOH-MWCNTs nanocomposite hydrogels) as shown in Table 1 and Figure 8, where the Freundlich model showed a high agreement with the adsorption data at equilibrium, which is evident from the value of correlation coefficient (R^2) = 0.9841 for lead Pb(II). Free isotherms indicate the homogeneous nature of the surface and that active sites are present on the superposition surface, which

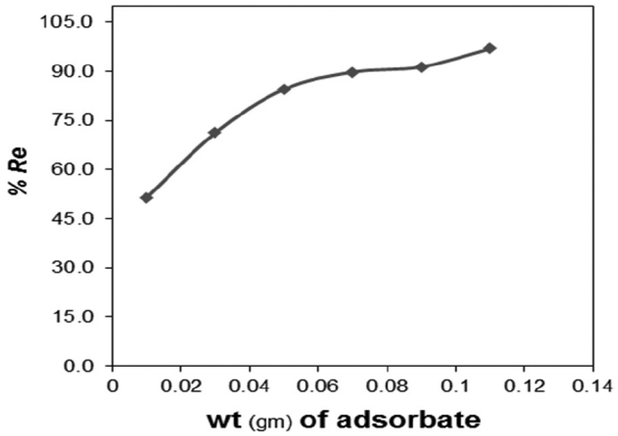

Figure 7: Effect of weight on the removal of Pb(II) ions.

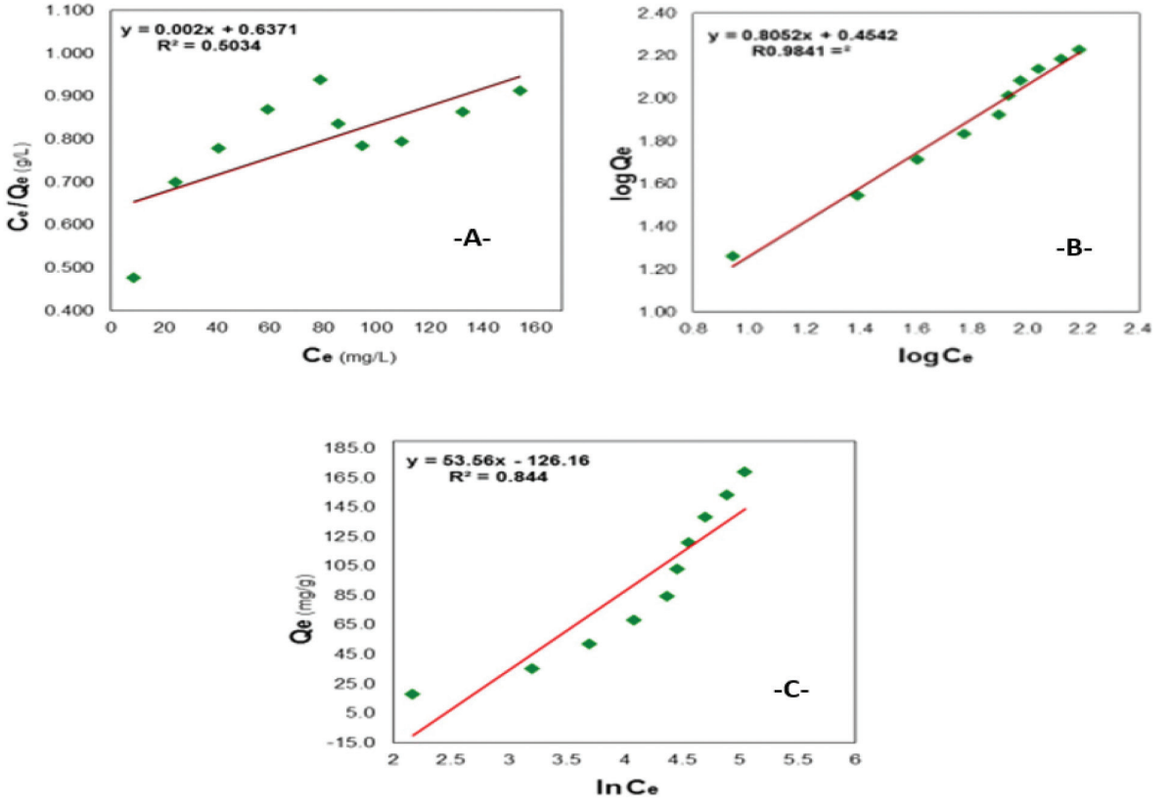

Figure 8: Adsorption isotherm models for lead Pb(II) (A) Langmuir, (B) Freundlich, and (C) Temkin model.

have equal energy, as indicated by the formation of a monolayer of adsorbed particles. The Freundlich isothermal model is valid for multilayer adsorption of a dense material on the surface of a heterogeneous absorbent material (Xue et al., 2017).

Table 1: Langmuir, Freundlich, and Temkin isotherm models for the Pb(II) adsorption

lang	R^2	q_m	K_L
	0.5034	500	0.00314
Frend.	0.9841	**n**	$\mathbf{K_F}$
		1.241927471	2.84577
Temk.	0.844	**B**	$\mathbf{K_T}$
		53.56	0.09485

Impact of Temperature and Calculation of Thermodynamic Functions

Temperature is one of the factors that significantly influence the adsorption process, where temperature changes can either enhance or decrease the ability to adsorb Pb(II) ions from the aqueous solution. The adsorption of Pb (II) ions was studied within the thermal range of 20 to 35 and through this study, the thermodynamic functions of the adsorption process were determined. The results showed that the amount of Pb(II) ions adsorbed on the composite surface the adsorption process escalates with increasing temperature, indicating that the adsorption process is exothermic, as shown in Figure 9. These findings are important for understanding how the adsorption process can be optimised by controlling the temperature. When the temperature increases, the adsorbed molecules gain more kinetic energy, which increases their dispersion. This leads to an increase in the system's entropy (ΔS) and therefore an increase in chaos or randomness in the distribution of Pb(II) ions molecules on the surface of the adsorbent material. Consequently, the attraction forces between the Pb(II) ions molecules and the available active sites for adsorption on the composite surface may weaken. In addition, increased temperature causes an expansion in the adsorbent surface's internal structure, facilitating the diffusion of the adsorbed Pb(II) ions within the adsorbent surface pores. Therefore, Pb(II) ions initially spread on the pore surface and increasingly permeate deeper pores with rising temperature (Ito and Yachidate, 1992).

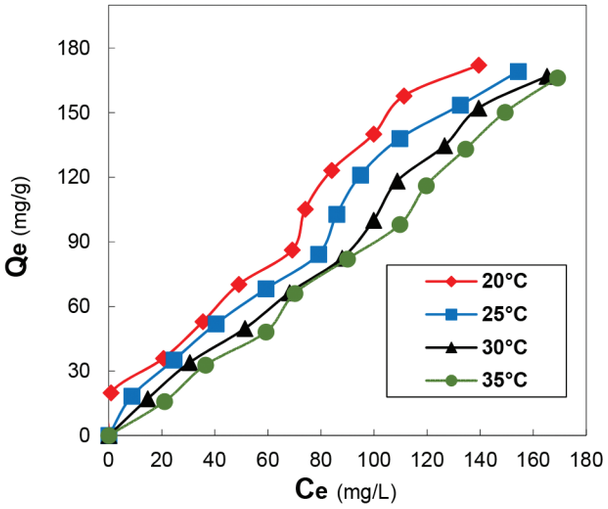

Figure 9: Isotherms representing Pd (II) adsorption onto (CMC-g-AAc)/COOH-MWCNTs nanocomposite hydrogel at various temperatures.

Thermodynamic functions such as enthalpy (ΔH), entropy (ΔS), and free energy (ΔG) provide valuable information about the nature of the process and whether it is spontaneous or not. The negative enthalpy (ΔH)= -0.022 value obtained and indicates that the process is exothermic, i.e., it generates heat. If the value is less than 40 KJ/mol, it usually indicates that the bonding is of a physical nature, which aligns with the results obtained. The positive entropy (ΔS) = 15.229 value indicates an increase in randomness or chaos in the system, suggesting that the molecules are free to move. A negative free energy (ΔG) = -4.538 value indicates that the process is spontaneous, i.e., it naturally occurs without the need to supply the system with energy. If the study aligns with these results, it confirms that the adsorption process of Pb (II) ions on the adsorbent surface is spontaneous and exothermic, with an increase in the system's disorder (Hosaman et al., 2012; Radia et al., 2022; Wankasi et al., 2005).

Effect of pH

This study involved fixing all conditions of temperature, equilibrium time, and the weight of the adsorbent, while varying the acid function. The latter factor has significant importance in the adsorption process due to its impacts on the interactions occurring between the molecules of the adsorbate and the surface of the adsorbent and on the adsorption capacity in general. Changing the acid function leads to the ionisation of the active functional groups of both the adsorbent and adsorbate models, which in turn changes the charge type, which could be either positive or negative (Figure 10).

In the acidic environment, an antagonistic interaction is observed between the hydrogen ions, which carry

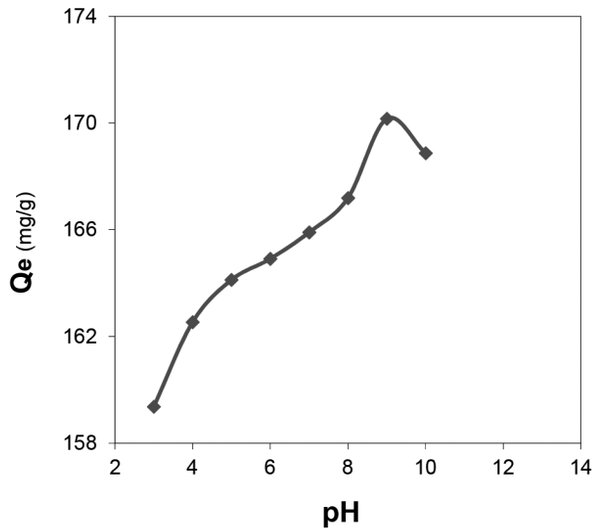

Figure 10: Impact of pH variations on Pb(II) ions adsorption by adsorbents at 25°C.

a positive charge, and the positively charged lead ions, resulting in a diminished adsorption process. It is noticed that the quantity of adsorption escalates in tandem with the pH augmentation (Figure 10) (Alkaim and Ajobree, 2020; Kislina et al., 2009).

Conclusion

We concluded that the best adsorption was done by using the prepared surface (CMC-g-AAc)/COOH-MWCNTs. The higher adsorption process reached equilibrium within 2 hrs, and the percentage of removal reaching to 82% of Pb(II) ions. The process followed a type (S4) isotherm and various isotherm models, suggesting effective Pb(II) ion monolayer adsorption. The endothermic adsorption process, reflected by thermodynamic calculations, improved at higher temperatures. Lower pH enhanced adsorption due to charge interactions, and salt additions boosted Pb(II) ion adsorption, with the most effective results observed with lower valency and larger salt ions.

References

Aljeboree, A.M. and A. Alkaim (2019). Comparative removal of three textile dyes from aqueous solutions by adsorption: As a model (corn-cob source waste) of plants role in environmental enhancement. *Plant Archives*, **19(1):** 1613-1620.

Aljeboree, A.M., Hussein, F.H. and A.F. Alkaim (2019). Removal of textile dye (methylene blue MB) from aqueous solution by activated carbon as a model (corn-cob source waste of plant): As a model of environmental enhancement. *Plant Archives*, **19:** 906-909.

Alkaim, A.F. and A.M. Ajobree (2020). White marble as an alternative surface for removal of toxic dyes (Methylene blue) from aqueous solutions. *International Journal of Advanced Science and Technology*, **29(5):** 5470-5479.

Alvares Rodrigues, L. and M.L.C. Pinto da Silva (2010). Adsorption kinetic, thermodynamic and desorption studies of phosphate onto hydrous niobium oxide prepared by reverse microemulsion method. *Adsorption-Journal of The International Adsorption Society*, **16(3):** 173-181.

Angevaare, P.A.J.M., Grootendorst, E.J., Zuur, A.P. and V. Ponec (1990). The adsorption of aliphatic nitrocompounds on oxides investigated by FT-IR spectroscopy. *Studies in Surface Science and Catalysis*, **55:** 861-868.

Assadi, A., Mohammadian Fazli, M., Emamjomeh, M.M. and M. Ghasemi (2016). Optimization of lead removal by electrocoagulation from aqueous solution using response surface methodology. *Desalination and Water Treatment*, **57(20):** 9375-9382.

Al-Mashhadani, Z.I., Aljeboree, A.M., Radia, N.D. and O.K.A. Alkadir (2021). Antibiotics removal by adsorption onto eco-friendly surface: Characterization and kinetic study, *International Journal of Pharmaceutical Quality Assurance*, **12(4):** 252-255.

Charpentier, T.V.J., Neville, A., Lanigan, J.L., Barker, R., Smith, M.J. and T. Richardson (2016). Preparation of magnetic carboxymethylchitosan nanoparticles for adsorption of heavy metal ions. *ACS Omega*, **1(1):** 77-83.

Havrdová, M., Poláková, K., Skopalik, J., Vujtek, M., Mokdad, A., Homolkova, M., Tucek, J., Nebesarova, J. and R. Zboril (2014). Field emission scanning electron microscopy (FE-SEM) as an approach for nanoparticle detection inside cells. *Micron*, **67:** 149-154.

Hosamani, M.T., Ayachit, N.H. and D.K. Deshpande (2012). Activation energy (ΔG*), enthalpy (ΔH*), and entropy (ΔS*) of some indoles and certain of their binary mixtures. *Journal of Thermal Analysis and Calorimetry*, **107(3):** 1301-1306.

Ito, K. and A. Yachidate (1992). Behavior of pertechnetate ion adsorption from aqueous solutions shown by activated carbons derived from different sources. *Carbon*, **30(5):** 767-771.

Kislina, I.S., Librovich, N.B. and S.G. Sysoeva (2009). The influence of sodium trifluoroacetate on the acidity function of solutions of trifluoroacetic acid in N,N-dimethylformamide. *Russian Journal of Physical Chemistry A*, **83(7):** 1111-1116

Kumar, M., Chung, J.S. and S.H. Hur (2019). Graphene composites for lead ions removal from aqueous solutions. *Applied Sciences*, **9(14):** 2925.

Lin, S.H., Lai, S.L. and H.G. Leu (2000). Removal of heavy metals from aqueous solution by chelating resin in a multistage adsorption process. *J Hazard Mater*, **76(1):**

139-53. doi: 10.1016/s0304-3894(00)00207-7. PMID: 10863020

Mohsen, A., Hemati, S. and M. Amiri (2015). Removal of lead ions from industrial wastewater: A review of removal methods. *International Journal of Epidemiologic Research*, **2(2):** 105-109.

Okamoto, T. and G. Meshitsuka (2003). Determination of the surface layer of kraft pulp fibers by field emission scanning electron microscopy (FE-SEM). *Japan Tappi Journal*, **57(10):** 1532-1536.

Plans, M., Wenstrup, M.J. and L.E. Rodriguez-Saona (2015). Application of infrared spectroscopy for characterization of dietary omega-3 oil supplements. *Journal of the American Oil Chemists' Society*, **92(7):** 957-966.

Radia, N.D., Aljeboree, A.M., Mahdi, A.B. and A.F. Alkai (2022). Eco-friendly synthesis of hydrogel nano-composites for removal of pollutants as a model Rose Bengal dye. *International Journal of Drug Delivery Technology*, **12(4):** 1527-1530.

Radia, N.D., Kamona, S.M.H., Jasem, H, Abass, R.R., Izzat, S.E., Ali, M.S., Ghafel, S.T. and A.M. Aljeboree (2022). Role of hydrogel and study of its high-efficiency to removal streptomycin drug from aqueous solutions. *International Journal of Pharmaceutical Quality Assurance*, **13(2):** 160-163.

Radia, N.D., Mahdi, A.B., Mohammed, G.A., Sajid, A., Altimari, U.S., Shams, M.A., Aljeboree, A.M. and F.H. Abdulrazzak (2022). Removal of Rose Bengal dye from aqueous solution using low cost (SA-g-PAAc) hydrogel: Equilibrium and kinetic study. *International Journal of Drug Delivery Technology*, **12(3):** 957-960.

Ricci, A., Olejar, K.J., Parpinello, G.P., Kilmartin, P.A and A. Versari (2015). Application of Fourier transform infrared (FTIR) spectroscopy in the characterization of tannins. *Applied Spectroscopy Reviews*, **50(5):** 407-442.

Sabri, M.M. (2020). Chemical and structural analysis of rocks using X-ray fluorescence and X-ray diffraction techniques. ARO. *The Scientific Journal of Koya University*, **8(1):** 79-87.

Sandeep, B.N. and S. Suresha (2013). Adsorption of Pb (II) from aqueous solution using NPP-modified bentonite as adsorbent. *Ecoscan*, **7(1-2):** 27-30.

Wankasi, D., Horsfall Jnr., M. and A.I. Spiff (2005). Retention of Pb (II) ion from aqueous solution by Nipah palm (*Nypa fruticans* wurmb) petiole biomass. *Journal of The Chilean Chemical Society*, **50(4):** 691-696.

Xue, L., Kang, Z., Caiyin, Y., Hui, P., Xiaoping, T. and F. Yanfeng (2017). Impact of contact time, pH, ionic strength, soil humic substances, and temperature on the uptake of Pb(II) onto graphene oxide. *Separation Science and Technology*, **52(6):** 987-996.

Zheng, S.Q., Liu, S.C., Zhang, P.Q., Yang, C. and T. Wang (2019). Adsorption of Cu2+, Zn2+, and Ni2+ Ions onto the adsorbent prepared from fluid catalytic cracking spent catalyst fines and diatomite. *Journal of Chemists and Engineers of Croatia*, **68(5-6):** 201-208.